EPS-0479
Submitted to Pa 10,17 and Pl 1,2,3
July 1995

Strangeness in Photoproduction and Deep Inelastic Scattering at HERA

H1 Collaboration

Abstract

The production of K^0 mesons is measured in photoproduction and deep inelastic positron-proton scattering interactions with the H1 detector at HERA. The K^0 multiplicities and differential cross-sections are compared with QCD-based Monte Carlo models which include leading order matrix elements and fragmentation effects. The production of strangeness is compared for diffractive and non-diffractive event samples. The suppression of strangeness production in fragmentation is discussed.

1 Introduction

The identification of K^0 particles in the hadronic final state of ep collisions at HERA is a method by which one can study the fragmentation of quarks and gluons into hadrons and more specifically the suppression of strange quarks relative to light quarks (u, d). In addition to this, a better understanding of the hadronisation phase is a potential step towards isolating strangeness that originates from the quark and gluon sea in the proton.

In this paper we present preliminary measurements of the K^0 production cross-sections in positron-proton interactions in photoproduction (γp) and deep inelastic scattering (DIS), defined as $Q^2 < 0.01\,\mathrm{GeV}^2$ and $Q^2 > 5\,\mathrm{GeV}^2$ respectively (see below).

For γp and DIS, we compare the production of K^0 in events with a large rapidity gap, interpreted as diffractive events, and without a large rapidity gap [1]. For this purpose, we define a ratio R as

$$R = \frac{N^{\mathrm{D}}_{K^0}}{N^{\mathrm{D}}_{(C)}} / \frac{N_{K^0}}{N_{(C)}}$$

where N_{K^0} is the number of K^0 and $N_{(C)}$ is the number of charged particles in the sample under consideration; the superscript D refers to diffractive events. The advantage of this double ratio is that it is rather insensitive to systematic effects.

In what follows, the pseudo-rapidity η of a particle is defined as

$$\eta = -\ln(\tan(\theta/2))$$

where θ is the polar angle of the particle with respect to the incident proton direction. Furthermore, p_t is defined as the momentum in the laboratory frame of a particle transverse to the beam axis.

Throughout this paper, a reference to K^0 will always mean $K^0 + \bar{K}^0$.

2 Event Selection

The data used for this analysis were taken in 1994 with the H1 detector [2] in collisions of 27.6 GeV positrons against 820 GeV protons; the corresponding integrated luminosity is about $1.2\,\mathrm{pb}^{-1}$ for the deep inelastic sample and about $1.4\,\mathrm{pb}^{-1}$ for the photoproduction sample.

The event selection is based on the identified scattered positron. A deep inelastic event is identified by requiring an electromagnetic cluster in the backward electromagnetic calorimeter; the kinematic range, calculated from the positron, has been restricted to

$$\begin{gathered} 0.0001 \leq x \leq 0.02 \\ 5\,\mathrm{GeV}^2 \leq Q^2 \leq 150\,\mathrm{GeV}^2 \\ 157^\circ < \theta_e < 173^\circ \\ E'_e > 12\,\mathrm{GeV} \\ W^2 > 3000\,\mathrm{GeV}^2 \\ y > 0.05 \end{gathered}$$

where x is the Bjorken scaling variable, Q^2 the negative squared four-momentum of the exchanged boson, θ_e is the angle of the scattered positron with respect to the direction of the incoming proton, E'_e is the energy of the scattered positron, W^2 is the total hadronic mass squared and y is

$$y = 1 - \frac{E'_e}{E_e} \sin^2 \frac{\theta_e}{2}$$

E_e being the energy of the incident positron.

The scattered positron of a photoproduction event is detected in the small-angle positron tagger, the accessible kinematic region being

$$Q^2 \leq 0.01\,\mathrm{GeV}^2$$
$$0.3 \leq y \leq 0.62$$

where the inelasticity y is approximated by

$$y = 1 - E'_e/E_e$$

E'_e is measured by the positron tagger and E_e is the energy of the incident positron. The photoproduction sample is constrained by a track-based trigger which demands at least one track in the Central Tracker.

In order to investigate the nature of diffractive phenomena, both samples were divided into diffractive and non-diffractive sub-samples. A diffractive event is defined as an event with a gap in rapidity dectected by requiring no any energy deposition in any of the H1 sub-detectors that extend beyond $\eta \geq 3.2$ [1]. The contamination of non-diffractive events in the diffractive samples is estimated to be less than 20%.

3 K^0 Selection

The K^0 particles are identified through the K^0_s decay channel

$$K^0_s \longrightarrow \pi^+\pi^-$$

Pairs of oppositely charged tracks reconstructed in the H1 Central Tracker are tested for consistency with a secondary vertex hypothesis. An attempt is made to fit both tracks to a common vertex under the constraints that the neutral particle originates from the primary interaction point and that momentum conservation holds at the decay vertex. After a successful fit, further cuts are applied in order to reduce the combinatorial background. The reconstructed kaons are then restricted to the kinematic range

$$0.25\,\mathrm{GeV}^2 \leq p_t^2 \leq 4.5\,\mathrm{GeV}^2$$
$$|\ \eta\ | \leq 1.3$$

for deep inelastic events and

$$0.25\,\mathrm{GeV}^2 \leq p_t^2 \leq 25\,\mathrm{GeV}^2$$
$$|\ \eta\ | \leq 1.3$$

for the photoproduction sample. The wider range in p_t^2 in photoproduction is made possible by higher statistics. Over this region the acceptance of the H1 Central Tracker for kaons, combined with the selection cuts, is well understood.

The observed spectra must be corrected for detector effects in order to obtain meaningful distributions. For the DIS sample the corrections applied to the observed spectra have been calculated by means of a detailed Monte Carlo simulation of the H1 detector. A detailed analysis of systematic effects has been performed. We estimate that the overall systematic uncertainty on the multiplicities is about 10%. The main sources of uncertainty are the selection cuts, the resolutions and the parameters assumed in the simulation and the method used to separate the K^0 from the background.

The corrections applied to the photoproduction spectra have been factorized, each contribution being studied independently. To calculate the losses due to the limited acceptance of the central jet chamber, its geometry has been modeled in order to determine a p_t- and η-dependent weight for each reconstructed K^0. This geometrical model was also used to estimate the losses caused by inefficient regions in the tracker which show up in a non-flat azimuthal distribution. Losses due to the secondary-vertex finder have been estimated using a detailed Monte Carlo simulation of the detector and the reconstruction. The efficiency of the trigger has been estimated by means of an independent reference trigger and by calculating an event probability derived from single-track efficiencies. The stability of the measurement has been studied by varying all cuts around their nominal value. The systematic uncertainty on the differential cross-section is typically of the order of 11%, but increases in the highest bin of the η-distribution up to 18%.

The final dipion mass spectra for the non-diffractive deep inelastic sample is shown in figure 1. There are about 1800 K_s^0 in the deep inelastic sample and about 26000 in the photoproduction sample. Both the fitted K_s^0 mass of $497.9 \pm 0.2\,(\text{stat.}) \pm 0.2\,(\text{syst.})$ MeV and measured lifetime of 86 ± 6 ps (stat.) are consistent with the current world averages [3].

4 Results and discussion

4.1 Deep inelastic scattering

Within the restricted kinematic region described in section 2, the preliminary total K^0 multiplicity per event for non-diffractive and diffractive scattering is measured to be

$$0.268 \pm 0.008\,(\text{stat.}) \pm 0.027\,(\text{syst.})$$
$$0.22 \pm 0.02\,(\text{stat.}) \pm 0.02\,(\text{syst.})$$

respectively. This corresponds to a preliminary total cross-section for K^0 production of

$$15.5 \pm 0.4\,(\text{stat.}) \pm 2.2\,(\text{syst.})\,\text{nb}$$

Extrapolating to the kinematic range of [4], the average number of K^0's per event is

$$0.270 \pm 0.008\,(\text{stat.}) \pm 0.032\,(\text{syst.})$$

for diffractive and non-diffractive events combined, to be compared with the value in [4]

$$0.289 \pm 0.015\,(\text{stat.}) \pm 0.014\,(\text{syst.})$$

Fully corrected laboratory p_t^2 and η spectra are shown in figure 2 for the non-diffractive sample. These are compared to phenomenological predictions of two Monte Carlo models. The first one, MEPS, combines leading-order QCD matrix elements with Parton Showers, as implemented in LEPTO [5]. The second one, CDM, is based on colour dipole radiation [6]; photon-gluon fusion events are not described in this model but are added at a rate given by QCD matrix elements [5]. Both programs use JETSET 7.3 [7] to model the hadronisation process. The parton density parameterization used is MRSH [8], which gives a good description of the HERA F_2 structure function measurements [9, 10].

Predictions are shown for Monte Carlo events generated with the default JETSET parameter settings. Also shown is the prediction of MEPS with the JETSET parameter PARJ(2) (which defines the suppression factor s/u) set at 0.2. The K^0 spectra seem to favour $s/u = 0.2$, though within the statistical and systematic errors they do not exclude the default value of 0.3. This observation of an over-estimation of the K^0 yield would be consistent with results from the E665 muon-nucleon deep inelastic scattering experiment at Fermilab [11] which favors a strangeness suppression factor of 0.2. It is of interest that DELPHI and OPAL, from studies of strangeness production in e^+e^- collisions, report values of 0.23 and 0.245 respectively [12, 13], although this estimate was obtained in conjunction with an estimate of other JETSET parameters controling the suppression of vector mesons.

Figure 3 shows the distribution of the fragmentation variable z which is defined as

$$z = (p_{K^0_{//}} + E_{K^0})/(2p_q)$$

where E_{K^0}, $p_{K^0_{//}}$ and p_q are defined as the K^0 energy, the K^0 laboratory momentum component parallel to the struck parton, and the laboratory momentum of the struck parton, respectively; the last two quantities are calculated from the virtual photon momentum under the asumption that the quark is massless and the proton momentum is large. The predictions from MEPS with s/u set at 0.2 and 0.3 are overlaid. Also shown is the predicted MEPS z spectrum of K^0s when strange quark production within hadronisation is explicitly inhibited. In this case K^0s come primarily from strange and charm sea quark interactions and photon gluon fusion; it can be seen that they contribute substantially to the tail of the z-distribution, whereas K^0s from hadronisation dominate at lower z.

A comparison of the K^0 to charged particle yield is made between diffractive and non-diffractive events. The ratio R, as defined in the Introduction, is shown in figure 4 as a function of W^2. This number is consistent with unity over the full range of W^2. Table 4.1 summarises the K^0 multiplicities in the different event classes from data and from Monte Carlo predictions.

4.2 Photoproduction

In the photoproduction kinematic range previously described, the inclusive K^0 production cross-section has been measured as a function of p_t and η. We have compared our results to various predictions of PYTHIA 5.7 (with multiple interactions included), generating a standard mixture of minimum bias events with all contributing photon components (VMD, direct and anomalous) as well as the elastic and diffractive components of the

Data-set	No. K^0 per event
Non-Diffractive DIS data	0.268±0.008±0.027
MEPS($PARJ(2) = 0.3$)	0.316
MEPS($PARJ(2) = 0.2$)	0.260
CDM($PARJ(2) = 0.3$)	0.314
Diffractive DIS data	0.22±0.02±0.02

Table 1: Preliminary average number of K^0 per event in DIS as measured by H1 and predicted by phenomenological models.

VMD-part included [14]. For the proton and the VMD-component of the photon the parton density parameterisations GRV LO [15] were chosen. In addition JETSET has been used for the hadronisation step and IJRAY [16] for the simulation of the QED vertex $e \longrightarrow e\gamma$.

These comparisons, for various strangeness suppression factors, are shown in figure 5. As is the case in inelastic scattering, the Monte Carlo prediction for $s/u = 0.2$ seems to agree better with the data. However, the measured η-distribution and that predicted by the Monte Carlo do not agree very well, particularly in the high η range, where the systematic uncertainty becomes large; this precludes a meaningful estimate of s/u from the current measurement.

In order to determine that part of strangeness production, which does not originate from fragmentation, s/u has been set to 0; as can be seen from figure 5, the Monte Carlo predicts that it is more significant at high p_t.

The ratio R is shown in figure 4 as a function of p_t. Within errors, it is seen to be consistent with unity; no significant difference in the K^0 yield is observed between diffractive and non-diffractive photoproduction.

5 Conclusions

The K^0 yield has been measured in deep inelastic scattering for both diffractive and non-diffractive events. Within the kinematic range described in section 2 , the deep inelastic cross-section for K^0 production is measured to be $15.5 \pm 0.5 \pm 2.2$ nb.

Kaons, in both photoproduction and deep inelastic scattering, originate predominantly from fragmentation, except for those with high z or high p_t, where non-fragmentation processes become significant.

For non-diffractive deep inelastic events, there is indication that the rate of K^0 production is somewhat over-estimated by the QCD models with which we have compared our data. Varying the strangeness suppression factor within the hadronisation model from 0.3 to 0.2 gives a better agreement, particularly at lower values of p_t^2. However, given the systematic errors, a strangeness suppression factor of 0.3 is not excluded.

A similar result has been observed in photoproduction where the measured cross-section has been compared to PYTHIA predictions. Systematic uncertainties, however, and the lack of agreement between the shape of the measured η-distribution and that predicted by the Monte Carlo model do not allow an unambiguous determination of strangeness suppression in hadronisation from these data.

Finally, the K^0 to charged particles ratio is found to be the same within errors in diffractive and non-diffractive events, both in deep inelastic scattering and photoproduction.

6 Acknowledgements

We are grateful to the HERA machine group whose outstanding efforts made this experiment possible. We appreciate the immense effort of the engineers and technicians who constructed and maintained the detector. We thank the funding agencies for their financial support of the experiment. We wish to thank the DESY directorate for the support and hospitality extended to the non-DESY members of the collaboration.

References

[1] H1 Collaboration, T. Ahmed et al., *Phys. Lett.* **B348** (1995) 681.

[2] H1 Collab., I. Abt et al., DESY preprint 93-103 (1993), to be published to Nucl. Instr. and Meth.

[3] Particle Data Group, I. Montanet et al., *Phys. Rev.* **D50** (1994) 1173.

[4] ZEUS Collaboration, M. Derrick et al., preprint DESY-95-084 (1995).

[5] G. Ingelman, *Proceedings of the 1991 Workshop on Physics at HERA, Vol. 3.* (1992) 1366.

[6] L. Lonnblad, *Comput. Phys. Comm.* **71** (1992) 15.

[7] B. Andersson et al., *Phys. Rep. 97* (1983) 31.

[8] A. D. Martin, W. J. Stirling and R.G. Roberts, *Proceedings of the Workshop on Quantum Field Theory and Theoretical Aspects of High Energy Physics, eds R. Geyer and E. M. Hgenfrita* (1983) 11.

[9] ZEUS Collaboration, M. Derrick et al., *Z. Phys.* **C65** (1995) 379.

[10] H1 Collaboration, T. Ahmed et al., *Nucl. Phys.* **B439** (1995) 471.

[11] E665 Collaboration, M.R. Adams et al., *Z. Phys.* **C61** (1994) 539.

[12] DELPHI Collaboration, P. Abreu et al., *Z. Phys.* **C65** (1995) 587.

[13] OPAL Collaboration, P.D. Acton et al., *Z. Phys.* **C56** (1992) 521.

[14] T. Sjostrand, *Computer Phys. Commun.* **82** (1994) 74 (and additional updates to the referenced manual)
G.A. Schuler et al., *Nucl. Phys.* **B407** (1993) 539

[15] M. Glück et al., *Z. Phys.* **C48** (1990) 471
M. Glück et al., *Z. Phys.* **C53** (1992) 127
M. Glück et al., *Z. Phys.* **C53** (1992) 651

[16] UCD/IIRPA, preprints 92-94(1992) and 93-10(1993)

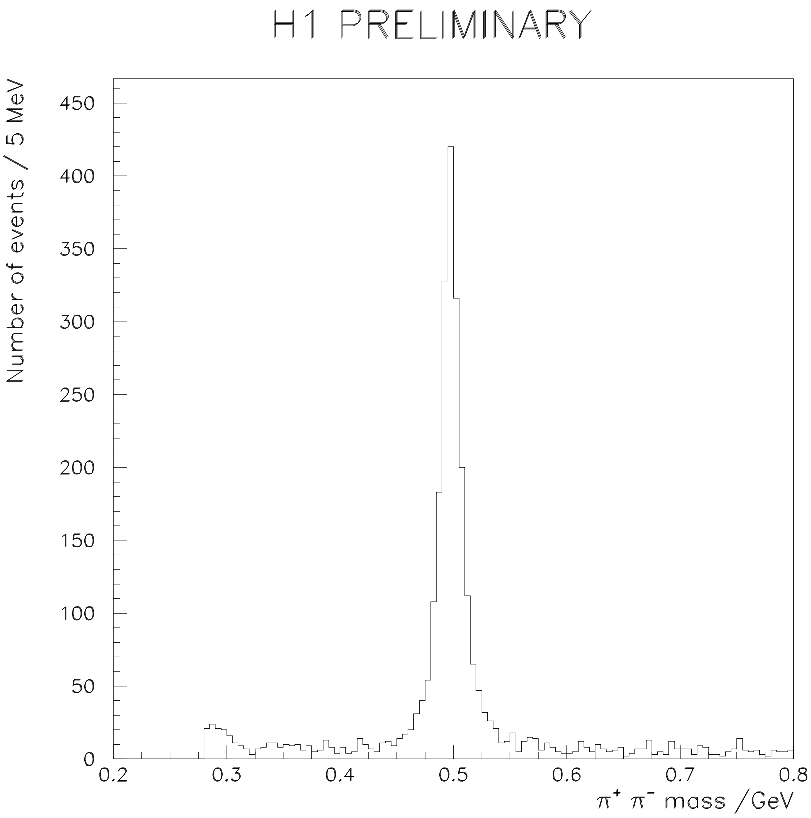

Figure 1: Dipion mass spectra after all K^0 selection cuts in deep inelastic scattering

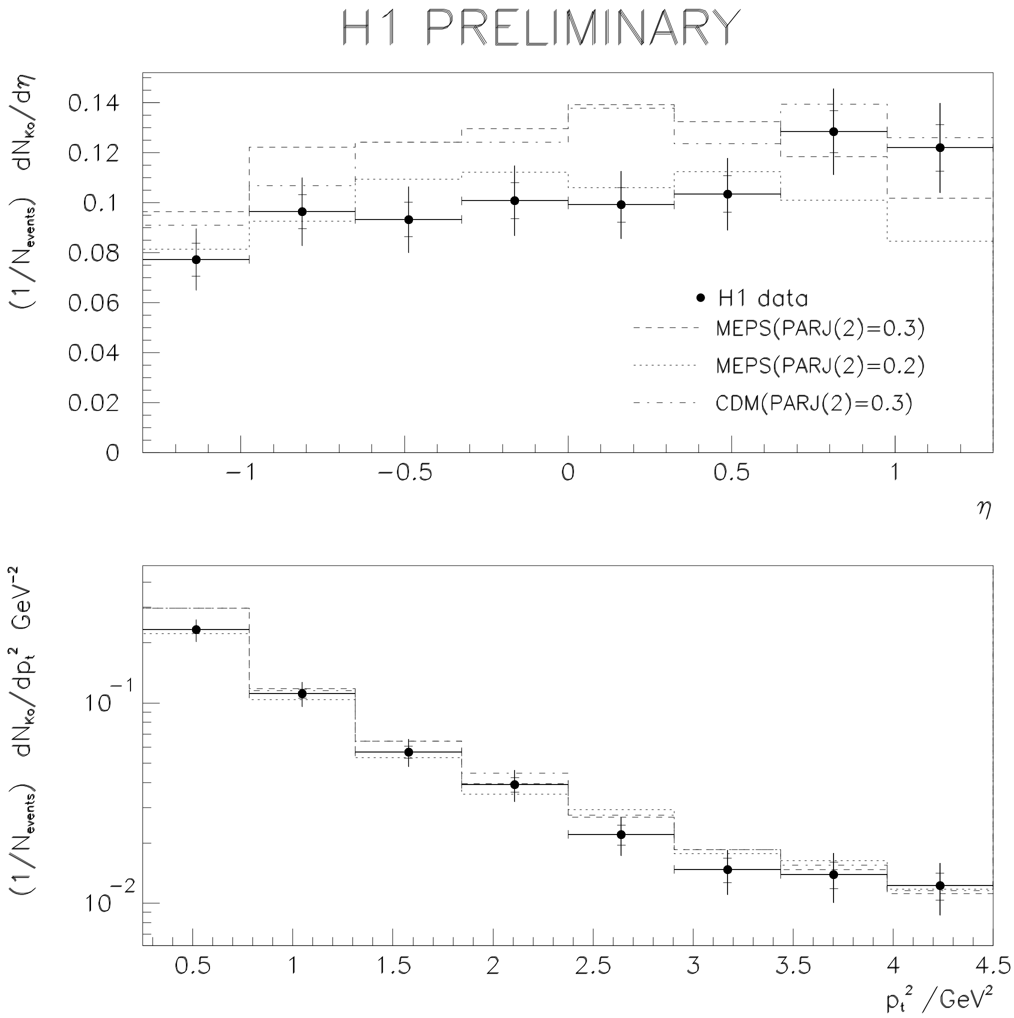

Figure 2: Corrected K^0 multiplicites in non-diffractive deep inelastic events as a function of η (top) and p_t^2 (bottom) compared to the predictions of MEPS and CDM Monte Carlos. The inner error bars are statistical and the outer bars contain the full statistical and systematic errors.

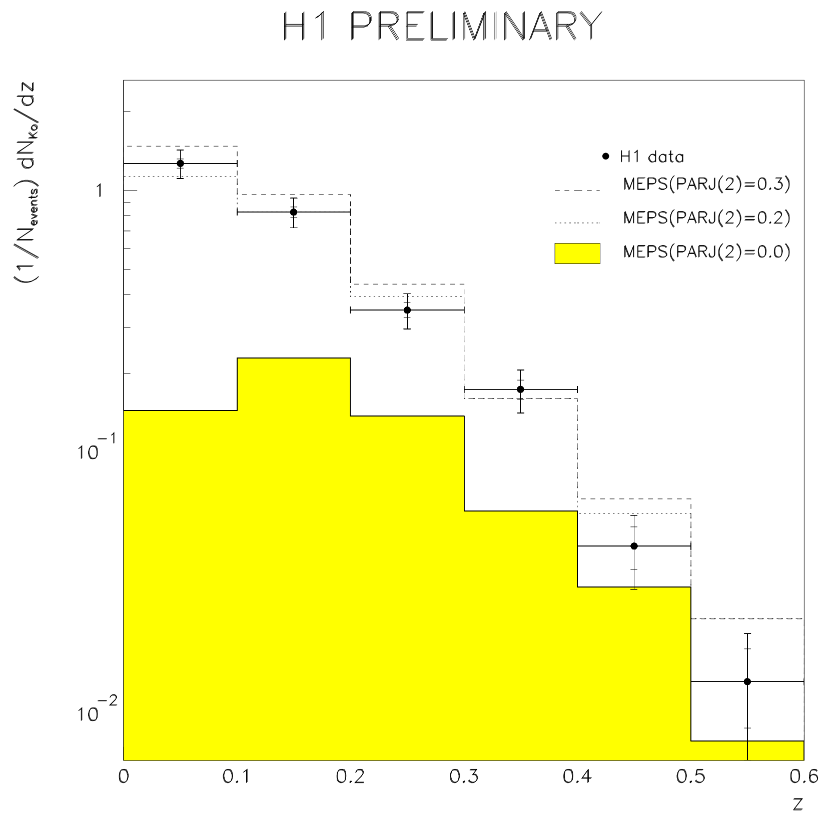

Figure 3: Corrected K^0 multiplicities in non-diffractive deep inelastic events as a function of the fragmentation variable z. Data are compared to MEPS for different values of the strangeness suppression factor. The inner error bars are statistical and the outer bars contain the full statistical and systematic errors

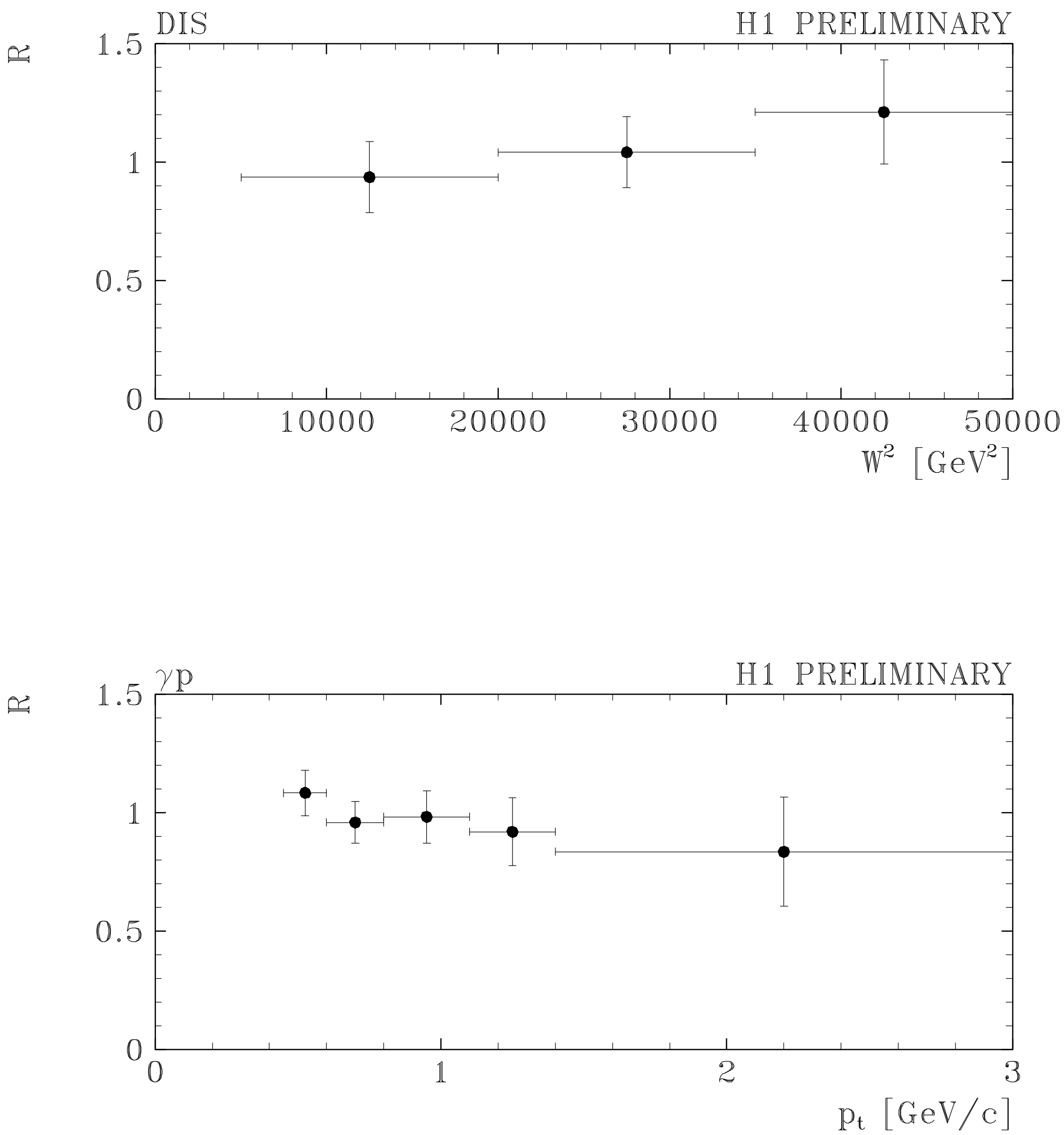

Figure 4: The double ratio $R = \frac{N^{\mathrm{D}}_{K^0}}{N^{\mathrm{D}}_{(C)}} / \frac{N_{K^0}}{N_{(C)}}$ (see Introduction) as a function of W^2 in deep inelastic scattering (top) and as a function of p_t in photoproduction (bottom).The error bars represent statistical errors.

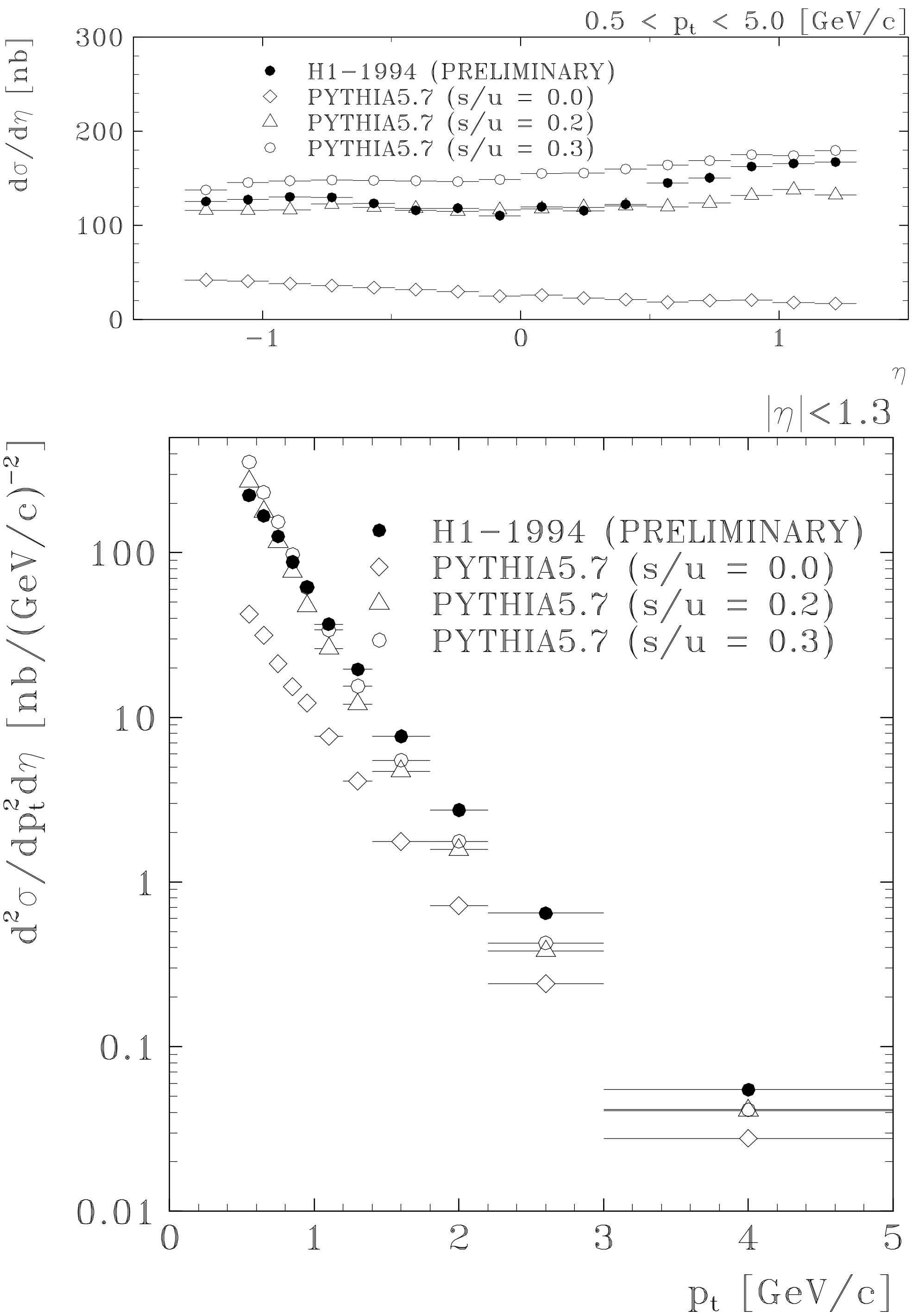

Figure 5: Inclusive K^0 photoproduction differential cross-sections as a function of pseudo-rapidity (top) and p_t (bottom). Data are compared to three PYTHIA 5.7 predictions for three s/u-suppression factors : 0, 0.2 and 0.3. In all cases multiple interactions effects have been included. Only the statistical errors are shown; the systematic errors are of the order of 11%, but go as high as 18% in the highest η-bin.